Supporting information for: High-throughput Computational Study of Halide Double Perovskite Inorganic Compounds

Yao Cai,[*,†] Wei Xie,[†] Yin Ting Teng,[‡] P.C. Harikesh,[¶] Biplab Ghosh,[¶] Patrick Huck,[§] Kristin A. Persson,[§,†] Nripan Mathews,[¶,‡] Subodh G. Mhaisalkar,[¶,‡] Matthew Sherburne,[†] and Mark Asta[*,†,‖]

†*Department of Materials Science and Engineering, University of California, Berkeley, California, USA*

‡*Energy Research Institute @ NTU (ERI@N), Interdisciplinary Graduate School, Nanyang Technological University, Singapore*

¶*School of Materials Science and Engineering, Nanyang Technological University, Singapore*

§*Energy Storage and Distributed Resources Division, Lawrence Berkeley National Laboratory, Berkeley, California, USA*

‖*Materials Sciences Division, Lawrence Berkeley National Laboratory, Berkeley, California, USA*

E-mail: yaocai@berkeley.edu; mdasta@berkeley.edu

Discussion on Tolerance Factor and Octahedral Factor

The approach used by Travis, et al.[S1] is more accurate in terms of screening perovskites using geometric criteria. It argues that Shannon radii were calculated from more ionic compounds

like fluorides and oxides, so are less suitable in more covalent compounds like bromides and iodides. Travis, et al then calculated 4 sets of ionic radii of several divalent metals for each of fluorides, chlorides, bromides and iodides, by surveying related compounds containing MX_6 octahedra in the ICSD. Using an approach similar to the above would require us to undertake a complete survey of related compounds containing MX_6 octahedra in ICSD, where M is a univalent or trivalent metal. Even though this is feasible, it requires additional work that lies beyond the scope of the current study.

As we use multiple screening steps (geometric criteria, energy above hull, band gap, effective mass), our goal is to reduce false negatives in each step. Here we argue that our current geometric screening uses a very relaxed criteria of tolerance factor and octahedral factor, in order to reduce false negatives. We allow some false positives in each of the screening steps.

Using the revised ionic radii for M-site cations, Travis et al set a criteria of octahedral factor $u > 0.41$ and tolerance factor $t > 0.875$[S1]. In general, the revised ionic radii for M-site cations would be smaller than the respective Shannon radii. Translating the above criteria to the situation using Shannon radii, we would end up with

$$u > \text{(a number larger than 0.41)} \tag{1}$$

$$t > \text{(a number smaller than 0.875)} \tag{2}$$

The current criteria we use for octahedral factor is $0.4 < u < 1.0$, so on the lower side, and it is thus more relaxed than criteria based on (1) and is better at reducing false negatives.

The current criteria we use for tolerance factor is $0.82 < t < 1.08$ where the lower bound is significant smaller than 0.875 and would probably satisfy the tolerance criteria even if we used a more realistic set of ionic radii.

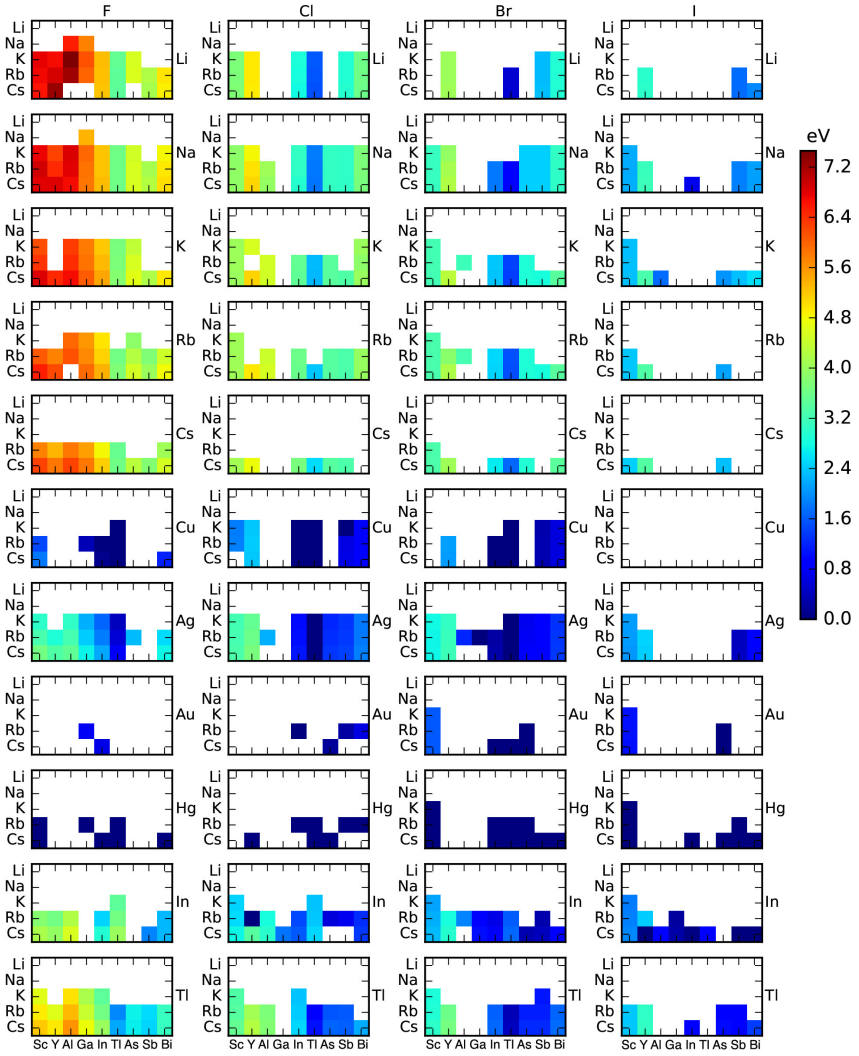

Figure S1: PBE band gaps for all halide $A_2MM'X_6$ compounds with energy above hull less than 50 meV/atom with A = Li, Na, K, Rb, Cs, M = Li, Na, K, Rb, Cs, Cu, Ag, Au, Hg, In, Tl, M′ = Sc, Y, Al, Ga, In, Tl, As, Sb, Bi, and X = F, Cl, Br, I.

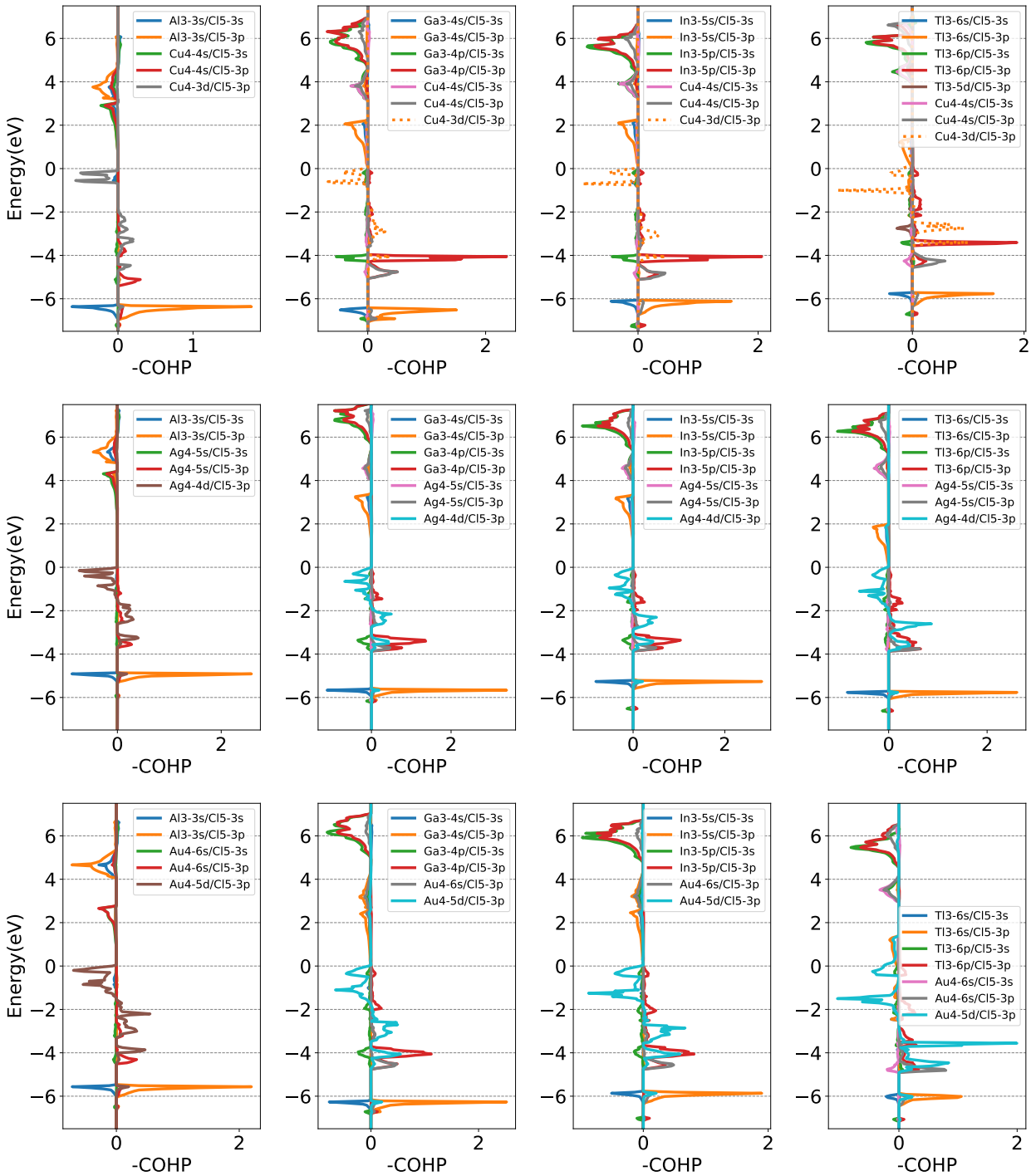

Figure S2: Negative crystal orbital Hamilton population(-COHP)[S2–S5], calculated by PBE for $Cs_2MM'Cl_6$ with M = Cu, Ag, Au and M′ = Al, Ga, In ,Tl.

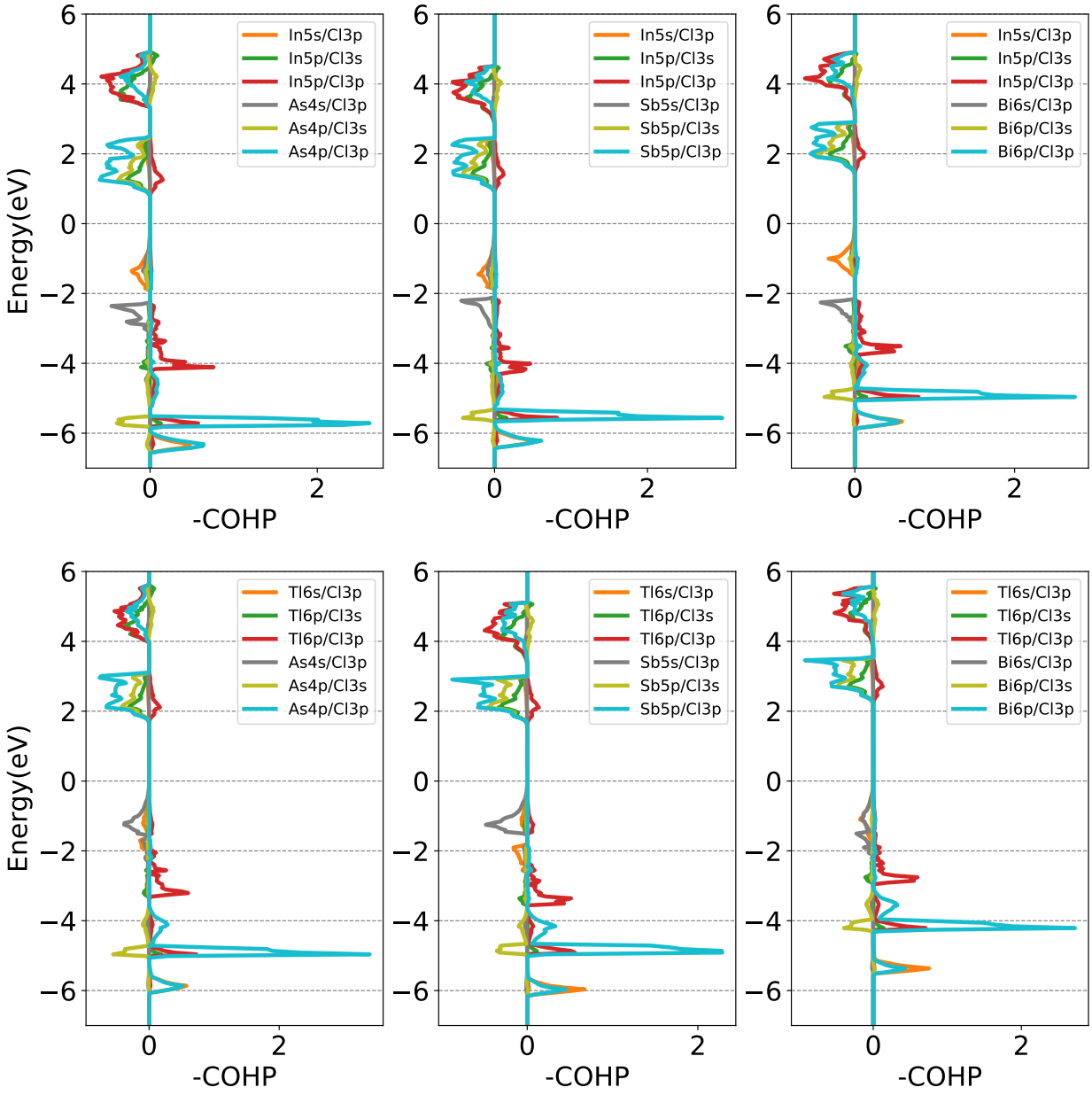

Figure S3: Negative crystal orbital Hamilton population(-COHP)[S2–S5], calculated by PBE for $Cs_2MM'Cl_6$ with M = In, Tl and M′ = As, Sb, Bi.

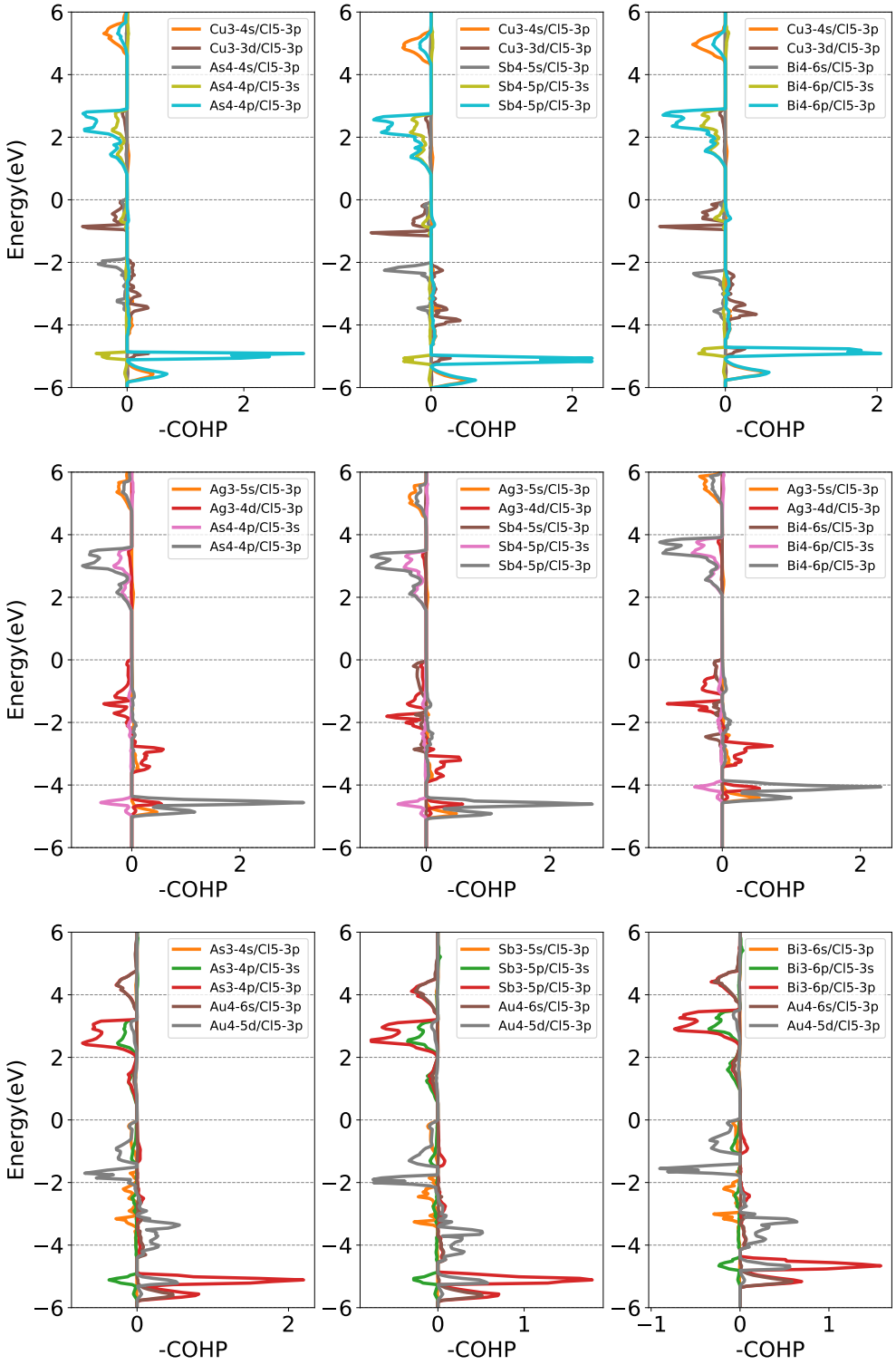

Figure S4: Negative crystal orbital Hamilton population(-COHP)[S2–S5], calculated by PBE for $Cs_2MM'Cl_6$ with M = Cu, Ag, Au and M′ = As, Sb, Bi.

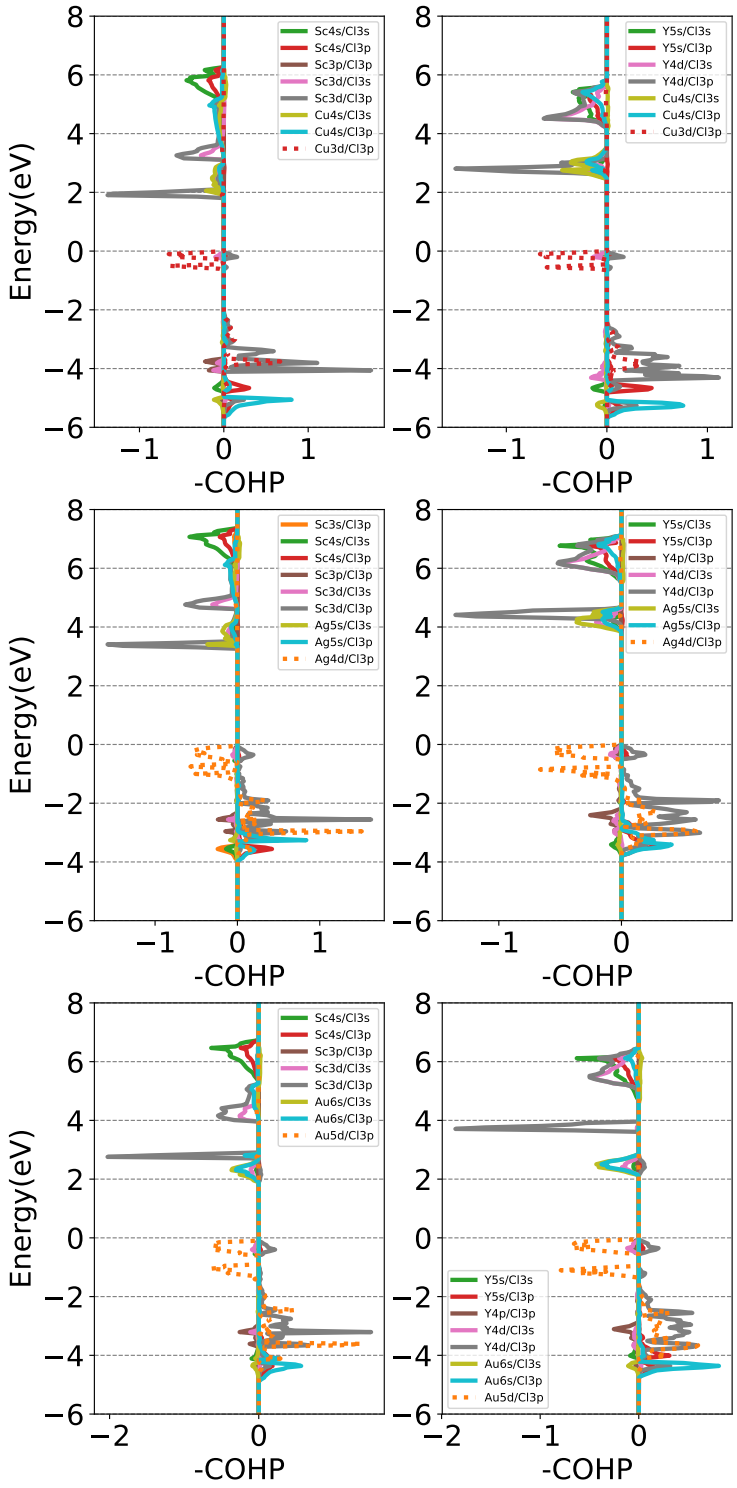

Figure S5: Negative crystal orbital Hamilton population(-COHP)[S2–S5], calculated by PBE for $Cs_2MM'Cl_6$ with M = Cu, Ag, Au and M′ = Sc, Y.

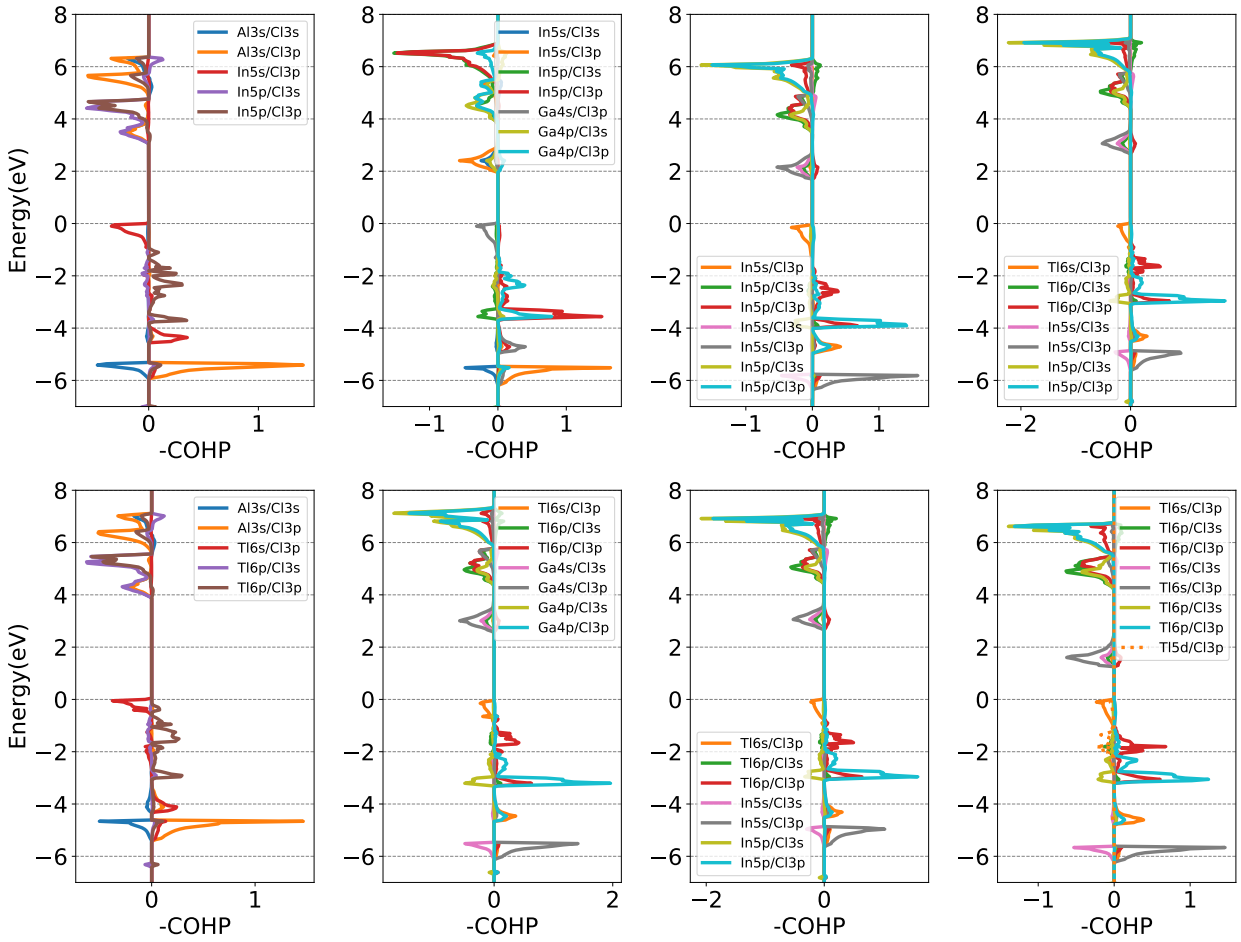

Figure S6: Negative crystal orbital Hamilton population(-COHP)[S2–S5], calculated by PBE for $Cs_2MM'Cl_6$ with M = In, Tl and M′ = Al, Ga, In, Tl.

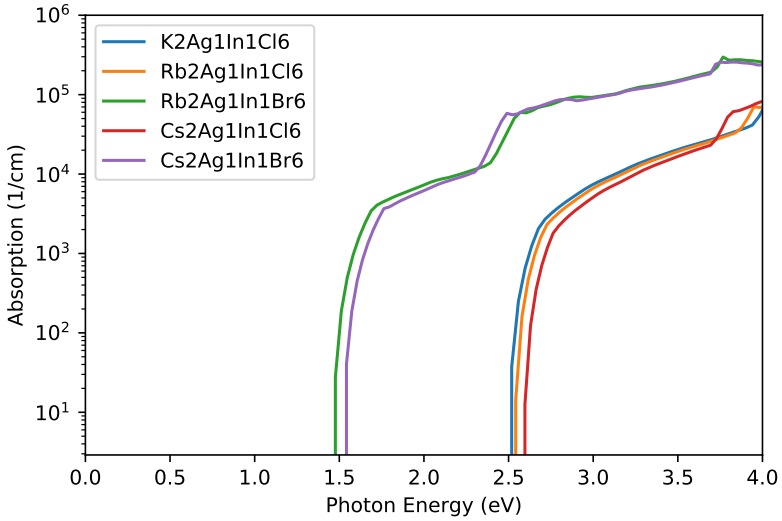

Figure S7: Calculated absorption spectra for halide $A_2MM'X_6$ compounds from Category 1.

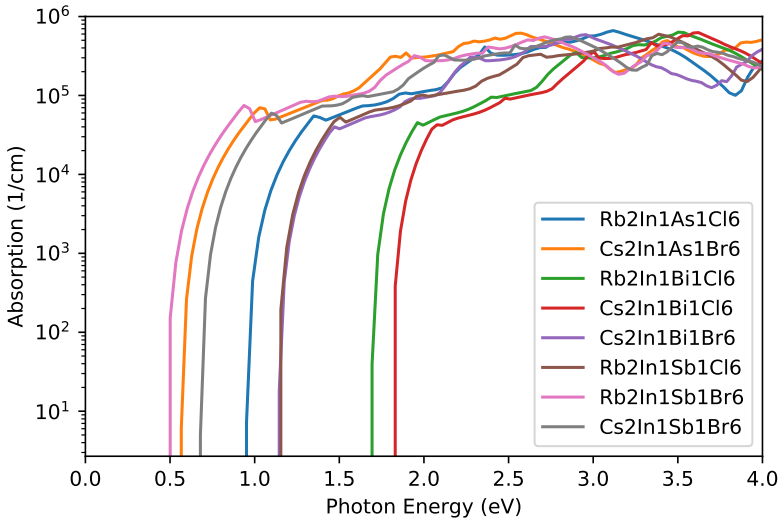

Figure S8: Calculated absorption spectra for halide $A_2MM'X_6$ compounds from Category 2.

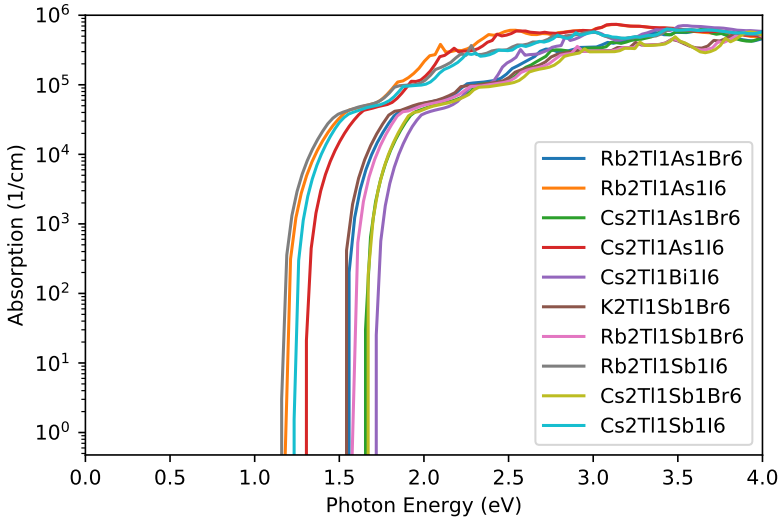

Figure S9: Calculated absorption spectra for halide $A_2MM'X_6$ compounds from Category 2.

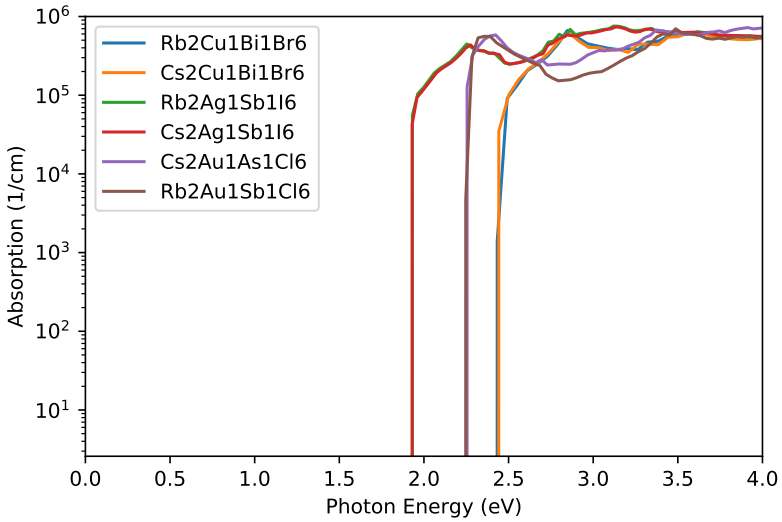

Figure S10: Calculated absorption spectra for halide $A_2MM'X_6$ compounds from Category 3.

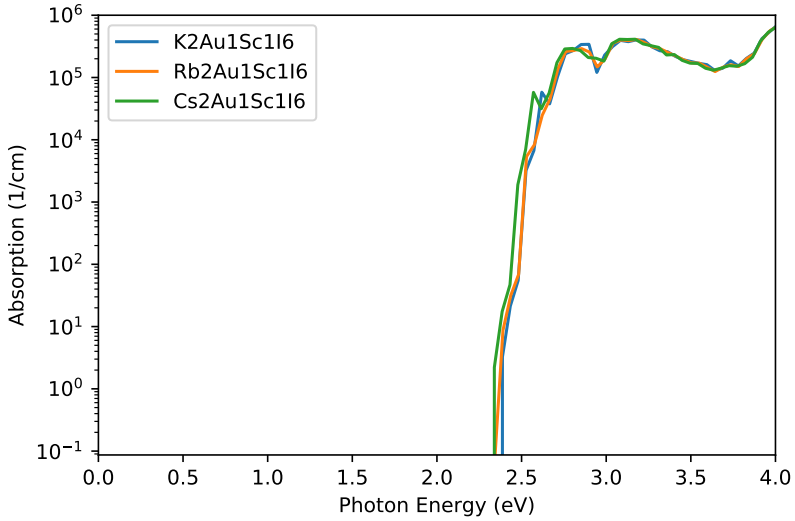

Figure S11: Calculated absorption spectra for halide $A_2MM'X_6$ compounds from Category 4.

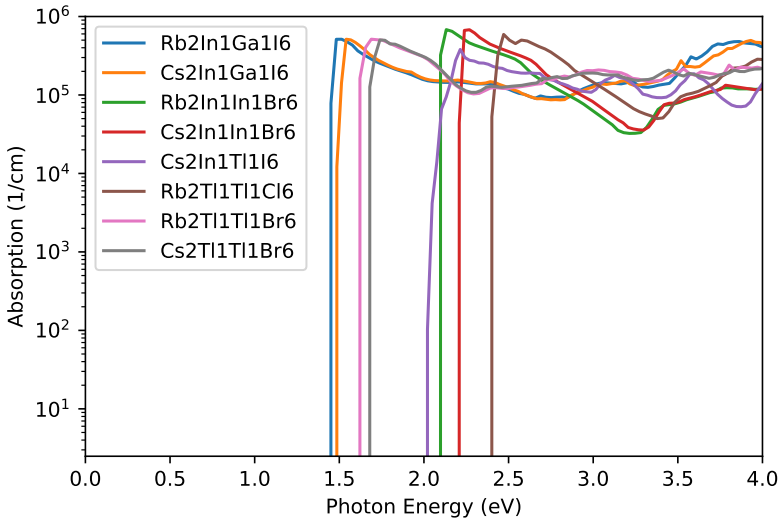

Figure S12: Calculated absorption spectra for halide $A_2MM'X_6$ compounds from Category 5.

Table S1: 79 $A_2MM'X_6$ compounds experimentally reported in the ICSD with A^{1+}, M^{1+}, M'^{3+} and X^{1-} ions. Chemical formula, ICSD collection codes, space groups, crystal systems, and number of atoms per unit cell are listed.

Formula	**ICSD ID**	**Space Group**	**Crystal System**	**Nsites**
$Cs_2AgAuCl_6$	[26162]	I4/mmm	Tetragonal	10
$Cs_2AgAuCl_6$	[24516]	$Fm\bar{3}m$	Cubic	10
$Cs_2AgBiBr_6$	[252164, 291597, 239875]	$Fm\bar{3}m$	Cubic	10
$Cs_2AgBiCl_6$	[291598, 239874, 252451]	$Fm\bar{3}m$	Cubic	10
Cs_2KBiF_6	[9383]	$Fm\bar{3}m$	Cubic	10
Cs_2KCoF_6	[6037]	$Fm\bar{3}m$	Cubic	10
Cs_2KCrF_6	[9705]	$Fm\bar{3}m$	Cubic	10
Cs_2KEuCl_6	[84845]	$Fm\bar{3}m$	Cubic	10
Cs_2KFeF_6	[42144]	$Fm\bar{3}m$	Cubic	10
Cs_2KMoF_6	[4053]	$Fm\bar{3}m$	Cubic	10
Cs_2KRhF_6	[4056]	$Fm\bar{3}m$	Cubic	10
Cs_2KScCl_6	[59196]	$Fm\bar{3}m$	Cubic	10
Cs_2KSmCl_6	[166519]	$Fm\bar{3}m$	Cubic	10
Cs_2KTbCl_6	[84844]	$Fm\bar{3}m$	Cubic	10
Cs_2KYF_6	[25367, 155977]	$Fm\bar{3}m$	Cubic	10
Cs_2LiGaF_6	[9004]	$P\bar{3}m1$	Trigonal	10
$Cs_2LiInCl_6$	[65735]	$R\bar{3}m$	Trigonal	20
$Cs_2LiLuCl_6$	[59194]	$Fm\bar{3}m$	Cubic	10
$Cs_2LiScCl_6$	[65734]	$R\bar{3}m$	Trigonal	20
Cs_2LiYCl_6	[65731]	$Fm\bar{3}m$	Cubic	10
Cs_2NaAlF_6	[93459, 200305, 41801, 93458]	$R\bar{3}m$	Trigonal	20
$Cs_2NaBiCl_6$	[59195, 2738]	$Fm\bar{3}m$	Cubic	10
Cs_2NaBiF_6	[9382]	$Fm\bar{3}m$	Cubic	10
$Cs_2NaCeCl_6$	[85021]	$Fm\bar{3}m$	Cubic	10
Cs_2NaCoF_6	[42157]	$R\bar{3}m$	Trigonal	20
Cs_2NaCrF_6	[200, 9002]	$R\bar{3}m$	Trigonal	20
$Cs_2NaErCl_6$	[50361]	$Fm\bar{3}m$	Cubic	10
Cs_2NaErF_6	[23143]	$Fm\bar{3}m$	Cubic	10
Cs_2NaFeF_6	[16255, 9003, 201]	$R\bar{3}m$	Trigonal	20
Cs_2NaFeF_6	[65503]	$Fm\bar{3}m$	Cubic	10
Cs_2NaGaF_6	[55003, 55698]	$R\bar{3}m$	Trigonal	20
$Cs_2NaHoCl_6$	[245367, 245366]	$Fm\bar{3}m$	Cubic	10
Cs_2NaInF_6	[24921]	$Fm\bar{3}m$	Cubic	10
$Cs_2NaLaBr_6$	[426112]	$Fm\bar{3}m$	Cubic	10
$Cs_2NaLaCl_6$	[425945]	$Fm\bar{3}m$	Cubic	10
Cs_2NaScF_6	[22116, 55694]	$Fm\bar{3}m$	Cubic	10
$Cs_2NaSmCl_6$	[50363]	$Fm\bar{3}m$	Cubic	10
$Cs_2NaTbCl_6$	[96062]	$Fm\bar{3}m$	Cubic	10
Cs_2NaTlF_6	[22118]	$Fm\bar{3}m$	Cubic	10
Cs_2NaYBr_6	[65733]	$Fm\bar{3}m$	Cubic	10

Table S1 – continued from previous page

Formula	ICSD ID	Space Group	Crystal System	Nsites
Cs_2NaYCl_6	[245353, 65732, 245354]	$Fm\bar{3}m$	Cubic	10
Cs_2NaYF_6	[25368]	$Fm\bar{3}m$	Cubic	10
$Cs_2NaYbCl_6$	[50362]	$Fm\bar{3}m$	Cubic	10
Cs_2RbBiF_6	[9384]	$Fm\bar{3}m$	Cubic	10
Cs_2RbYF_6	[25366]	$Fm\bar{3}m$	Cubic	10
Cs_2TlBiF_6	[9385]	$Fm\bar{3}m$	Cubic	10
Cs_2TlFeF_6	[6036]	$Fm\bar{3}m$	Cubic	10
Cs_2TlMoF_6	[15772]	$Fm\bar{3}m$	Cubic	10
$K_2CsBiCl_6$	[201983]	C2/c	Monoclinic	40
K_2LiAlF_6	[408552, 48149]	$R\bar{3}m$	Trigonal	20
K_2LiAlF_6	[37250, 408553]	$Fm\bar{3}m$	Cubic	10
K_2LiAlF_6	[27672]	$P\bar{3}m1$	Trigonal	30
K_2NaAlF_6	[34201, 164216, 40886, 22109, 6027]	$Fm\bar{3}m$	Cubic	10
K_2NaCrF_6	[40965, 22199]	$Fm\bar{3}m$	Cubic	10
K_2NaFeF_6	[61277, 22200]	$Fm\bar{3}m$	Cubic	10
K_2NaInF_6	[23430, 22113]	$Fm\bar{3}m$	Cubic	10
K_2NaMoF_6	[15777]	$Fm\bar{3}m$	Cubic	10
K_2NaRhF_6	[27342]	$Fm\bar{3}m$	Cubic	10
K_2NaScF_6	[22112, 65730]	$Fm\bar{3}m$	Cubic	10
K_2NaTlF_6	[22114]	$Fm\bar{3}m$	Cubic	10
K_2NaYF_6	[22115]	$Fm\bar{3}m$	Cubic	10
Na_2LiAlF_6	[280906, 96477]	$P2_1/c$	Monoclinic	20
Rb_2KBiF_6	[9387]	$Fm\bar{3}m$	Cubic	10
$Rb_2LiDyBr_6$	[402536]	$Fm\bar{3}m$	Cubic	10
Rb_2LiFeF_6	[16400]	$R\bar{3}m$	Trigonal	20
Rb_2LiGaF_6	[50468]	$R\bar{3}m$	Trigonal	20
Rb_2NaAlF_6	[290318]	$Fm\bar{3}m$	Cubic	10
Rb_2NaBiF_6	[9386]	$Fm\bar{3}m$	Cubic	10
Rb_2NaCoF_6	[42148]	$Fm\bar{3}m$	Cubic	10
Rb_2NaCrF_6	[9706]	$Fm\bar{3}m$	Cubic	10
Rb_2NaErF_6	[23142]	$Fm\bar{3}m$	Cubic	10
Rb_2NaFeF_6	[42146, 4030, 40966]	$Fm\bar{3}m$	Cubic	10
Rb_2NaHoF_6	[86274]	I4/m	Tetragonal	10
Rb_2NaHoF_6	[86273]	$Fm\bar{3}m$	Cubic	10
Rb_2NaMoF_6	[15774]	$Fm\bar{3}m$	Cubic	10
Rb_2NaRhF_6	[27341]	$Fm\bar{3}m$	Cubic	10
$Rb_2NaTmCl_6$	[200549, 200550]	$Fm\bar{3}m$	Cubic	10
Rb_2NaYF_6	[25369]	$Fm\bar{3}m$	Cubic	10
Tl_2NaRhF_6	[27340]	$Fm\bar{3}m$	Cubic	10

Table S2: Calculated lattice parameters of the 30 $A_2MM'X_6$ compounds identified in the initial screening for candidate solar absorber materials. The second and third columns list calculated results obtained by semi-local GGA-PBE and hybrid HSE06 functionals, respectively, and the last column lists calculated results from the literature. All compounds are cubic with space group $Fm\bar{3}m$.

	a ($\AA$)		
Compound	**GGA-PBE**	**HSE06**	**GGA-PBE from literature**
$K_2AgInCl_6$	10.50	10.43	
$Rb_2AgInCl_6$	10.57	10.49	
$Rb_2AgInBr_6$	11.14	11.05	
$Cs_2AgInCl_6$	10.68	10.60	
$Cs_2AgInBr_6$	11.22	11.16	
$Rb_2InAsCl_6$	10.92	10.83	
$Cs_2InAsBr_6$	11.51	11.43	
$Rb_2InBiCl_6$	11.41	11.35	
$Cs_2InBiCl_6$	11.48	11.42	11.44[S6]
$Cs_2InBiBr_6$	11.95	11.89	11.93[S6]
$Rb_2InSbCl_6$	11.26	11.20	
$Rb_2InSbBr_6$	11.77	11.69	
$Cs_2InSbBr_6$	11.83	11.76	11.80[S6]
$Rb_2TlAsBr_6$	11.58	11.50	
$Cs_2TlAsBr_6$	11.66	11.58	
Cs_2TlAsI_6	12.42	12.34	
Cs_2TlBiI_6	12.85	12.79	12.84[S6]
$Cs_2TlSbBr_6$	11.97	11.90	11.94[S6]
Cs_2TlSbI_6	12.72	12.66	12.72[S6]
$Cs_2AuAsCl_6$	10.54	10.48	
$Rb_2AuSbCl_6$	10.75	10.68	
K_2AuScI_6	11.81	11.77	
Rb_2AuScI_6	11.86	11.81	
Cs_2AuScI_6	11.92	11.87	
Cs_2InGaI_6	12.23	12.14	
$Rb_2InInBr_6$	11.61	11.56	
$Cs_2InInBr_6$	11.67	11.63	
$Rb_2TlTlCl_6$	11.26	11.16	
$Rb_2TlTlBr_6$	11.80	11.68	
$Cs_2TlTlBr_6$	11.87	11.74	

Table S3: 30 $A_2MM'X_6$ compounds identified in the screening for candidate solar absorber materials. Chemical formula, HSE+SOC calculated band gaps (E_g) and direct band gaps (direct E_g), band gap type(direct or indirect), measured band gaps and HSE+SOC calculations from the literature are listed. Asterisk(*) indicates HSE calculation without SOC.

	This work			**Experiment**	**Previous calculations**
Compound	**E_g(eV)**	**direct E_g(eV)**	**gap type**	**E_g(eV)**	**E_g(eV)**
$K_2AgInCl_6$	2.49	2.49	direct		
$Rb_2AgInCl_6$	2.52	2.52	direct		
$Rb_2AgInBr_6$	1.44	1.44	direct		
$Cs_2AgInCl_6$	2.57	2.57	direct	3.30[S7]	2.6*[S7]
$Cs_2AgInBr_6$	1.49	1.49	direct		
$Rb_2InAsCl_6$	0.74	0.74	direct		
$Cs_2InAsBr_6$	0.36	0.36	direct		
$Rb_2InBiCl_6$	0.79	0.79	direct		
$Cs_2InBiCl_6$	0.92	0.92	direct		0.91[S6], 0.88[S8]
$Cs_2InBiBr_6$	0.29	0.29	direct		0.0[S6], 0.33[S8]
$Rb_2InSbCl_6$	0.77	0.77	direct		
$Rb_2InSbBr_6$	0.20	0.20	direct		
$Cs_2InSbBr_6$	0.33	0.33	direct		0.41[S6], 0.41[S8]
$Rb_2TlAsBr_6$	1.11	1.11	direct		
$Cs_2TlAsBr_6$	1.23	1.23	direct		
Cs_2TlAsI_6	0.79	0.79	direct		
Cs_2TlBiI_6	0.66	0.66	direct		0.78[S6]
$Cs_2TlSbBr_6$	1.11	1.11	direct		1.25[S6]
Cs_2TlSbI_6	0.64	0.64	direct		0.81[S6]
$Cs_2AuAsCl_6$	0.90	2.36	indirect		
$Rb_2AuSbCl_6$	0.95	2.36	indirect		
K_2AuScI_6	1.82	2.13	indirect		
Rb_2AuScI_6	1.81	2.11	indirect		
Cs_2AuScI_6	1.78	2.09	indirect		
Cs_2InGaI_6	0.76	1.60	indirect		
$Rb_2InInBr_6$	1.43	2.17	indirect		
$Cs_2InInBr_6$	1.57	2.30	indirect		
$Rb_2TlTlCl_6$	1.83	2.51	indirect		
$Rb_2TlTlBr_6$	0.99	1.73	indirect		
$Cs_2TlTlBr_6$	1.07	1.79	indirect		

Table S4: 30 $A_2MM'X_6$ compounds identified from screening for candidate solar absorber materials. Chemical formula, energy above hull(E_{hull}), calculated effective masses for electrons (m_e) and holes (m_h) from this work and from the literature are listed.

	This work			**Previous calculations**	
Compound	**E_{hull}(eV/atom)**	**m_e**	**m_h**	**m_e**	**m_h**
$K_2AgInCl_6$	0.006	0.29	0.83		
$Rb_2AgInCl_6$	0.000	0.28	0.85		
$Rb_2AgInBr_6$	0.005	0.18	0.68		
$Cs_2AgInCl_6$	0.000	0.29	0.90		
$Cs_2AgInBr_6$	0.000	0.18	0.71		
$Rb_2InAsCl_6$	0.031	0.39	0.09		
$Cs_2InAsBr_6$	0.026	0.30	0.05		
$Rb_2InBiCl_6$	0.000	0.39	0.17		
$Cs_2InBiCl_6$	0.014	0.39	0.18	0.39[S6]	0.17[S6]
$Cs_2InBiBr_6$	0.000	0.32	0.11	0.3[S6]	0.11[S6]
$Rb_2InSbCl_6$	0.000	0.39	0.11		
$Rb_2InSbBr_6$	0.028	0.31	0.05		
$Cs_2InSbBr_6$	0.007	0.31	0.07	0.3[S6]	0.11[S6]
$Rb_2TlAsBr_6$	0.008	0.29	0.14		
$Cs_2TlAsBr_6$	0.000	0.31	0.15		
Cs_2TlAsI_6	0.000	0.23	0.13		
Cs_2TlBiI_6	0.023	0.24	0.17	0.23[S6]	0.18[S6]
$Cs_2TlSbBr_6$	0.012	0.31	0.16	0.3[S6]	0.2[S6]
Cs_2TlSbI_6	0.022	0.23	0.13	0.23[S6]	0.18[S6]
$Cs_2AuAsCl_6$	0.046	0.27	0.35		
$Rb_2AuSbCl_6$	0.048	0.28	0.34		
K_2AuScI_6	0.000	0.25	0.62		
Rb_2AuScI_6	0.000	0.24	0.63		
Cs_2AuScI_6	0.000	0.23	0.64		
Cs_2InGaI_6	0.018	0.22	0.51		
$Rb_2InInBr_6$	0.003	0.26	0.56		
$Cs_2InInBr_6$	0.000	0.27	0.58		
$Rb_2TlTlCl_6$	0.031	0.34	0.65		
$Rb_2TlTlBr_6$	0.026	0.25	0.55		
$Cs_2TlTlBr_6$	0.001	0.26	0.58		

Table S5: 30 $A_2MM'X_6$ compounds identified from screening for candidate solar absorber materials. Chemical formula, category, calculated SLME at L = $1\mu m$, PBE band gap(E_g), PBE direct dipole allowed band gap(E_g^{da}) for each compound are listed below.

Formula	**Category**	**SLME at $1\mu m$ (%)**	**E_g (eV)**	**E_g^{da} (eV)**
$Cs_2AgInCl_6$	1	5.44	2.58	2.58
$Rb_2AgInCl_6$	1	6.34	2.53	2.53
$K_2AgInCl_6$	1	6.83	2.49	2.49
$Cs_2AgInBr_6$	1	22.46	1.51	1.51
$Rb_2AgInBr_6$	1	23.36	1.45	1.45
$Rb_2InSbBr_6$	2	16.58	0.47	0.47
$Cs_2InAsBr_6$	2	20.20	0.56	0.56
$Cs_2InSbBr_6$	2	23.90	0.67	0.67
$Cs_2InBiCl_6$	2	24.92	1.81	1.81
Cs_2TlBiI_6	2	26.62	1.71	1.71
$Rb_2InBiCl_6$	2	27.23	1.69	1.69
$Cs_2TlAsBr_6$	2	27.70	1.65	1.65
$Cs_2TlSbBr_6$	2	27.73	1.65	1.65
$Rb_2TlAsBr_6$	2	29.28	1.54	1.54
$Rb_2InAsCl_6$	2	30.42	0.95	0.95
$Cs_2InBiBr_6$	2	31.87	1.14	1.14
$Rb_2InSbCl_6$	2	31.90	1.13	1.13
Cs_2TlAsI_6	2	32.08	1.30	1.30
Cs_2TlSbI_6	2	32.16	1.23	1.23
$Cs_2AuAsCl_6$	3	5.57	0.97	2.22
$Rb_2AuSbCl_6$	3	5.73	1.03	2.27
K_2AuScI_6	4	8.80	2.01	2.51
Rb_2AuScI_6	4	9.87	2.00	2.34
Cs_2AuScI_6	4	10.40	1.98	2.31
$Rb_2TlTlCl_6$	5	9.86	1.85	2.50
Cs_2InGaI_6	5	11.12	0.78	1.51
$Cs_2InInBr_6$	5	11.15	1.58	2.29
$Rb_2InInBr_6$	5	12.48	1.43	2.12
$Rb_2TlTlBr_6$	5	12.60	1.01	1.73
$Cs_2TlTlBr_6$	5	15.25	1.09	1.71

Table S6: 30 $A_2MM'X_6$ compounds identified from screening for candidate solar absorber materials. Chemical formula, category (see main text for definition), least stable phonon frequencies (f_{min}, THz), q-point of least stable phonon, least stable phonon frequencies at Γ ($f_{min,\Gamma}$, THz), energy difference between the cubic structure and the distorted structure induced by the imaginary phonon mode at Γ ($\Delta E = E_{cubic}$-$E_{distorted}$, meV/atom) and the space group of the distorted structure for each compound are listed. Note that negative frequencies represent the magnitude of imaginary frequencies for unstable phonons. For those compounds with missing entries in the sixth column, the magnitude of f_{min} and $f_{min,\Gamma}$ are large and they are considered unstable, so the energies of the distorted structures are not calculated.

Formula	**Category**	$\mathbf{f_{min}}$	**q-point**	$\mathbf{f_{min,\Gamma}}$	**ΔE**	**spacegroup**
$Cs_2AgInCl_6$	1	-0.00	Γ	-0.00	-0.02	
$Rb_2AgInCl_6$	1	-1.30	Γ	-1.30	5.25	$P\bar{1}$
$K_2AgInCl_6$	1	-1.84	Γ	-1.84	23.07	$P\bar{1}$
$Cs_2AgInBr_6$	1	-0.20	Γ	-0.20	-0.00	$P\bar{1}$
$Rb_2AgInBr_6$	1	-198.11	W	-170.47	NaN	P1
$Rb_2InSbBr_6$	2	-43.91	L	-31.74	NaN	$P\bar{1}$
$Cs_2InAsBr_6$	2	-0.00	Γ	0.00	-0.00	
$Cs_2InSbBr_6$	2	-0.52	Γ	-0.52	2.60	$P\bar{1}$
$Cs_2InBiCl_6$	2	-1.14	Γ	-1.14	8.23	$P\bar{1}$
Cs_2TlBiI_6	2	-0.64	Γ	-0.64	15.70	$P\bar{1}$
$Rb_2InBiCl_6$	2	-1.55	Γ	-1.55	31.75	$P\bar{1}$
$Cs_2TlAsBr_6$	2	-0.52	Γ	-0.52	1.61	$P\bar{1}$
$Cs_2TlSbBr_6$	2	-0.76	Γ	-0.76	8.98	$P\bar{1}$
$Rb_2TlAsBr_6$	2	-0.92	Γ	-0.92	17.06	$P\bar{1}$
$Rb_2InAsCl_6$	2	-137.94	Γ	-137.94	NaN	$Fm\bar{3}m$
$Cs_2InBiBr_6$	2	-0.70	Γ	-0.70	6.76	$P\bar{1}$
$Rb_2InSbCl_6$	2	-1.44	Γ	-1.44	23.01	$P\bar{1}$
Cs_2TlAsI_6	2	-0.44	Γ	-0.44	3.08	$P\bar{1}$
Cs_2TlSbI_6	2	-0.60	Γ	-0.60	10.52	$P\bar{1}$
$Cs_2AuAsCl_6$	3	-4.99	L	-0.00	0.02	
$Rb_2AuSbCl_6$	3	-3.51	L	-1.16	24.80	$P\bar{1}$
K_2AuScI_6	4	-243.35	L	-109.07	NaN	P1
Rb_2AuScI_6	4	-15.76	Γ	-15.76	NaN	P1
Cs_2AuScI_6	4	-0.54	L	-0.41	46.19	$P\bar{1}$
$Rb_2TlTlCl_6$	5	-1.61	Γ	-1.61	29.06	$P\bar{1}$
Cs_2InGaI_6	5	-0.38	Γ	-0.38	1.11	$P\bar{1}$
$Cs_2InInBr_6$	5	-0.56	Γ	-0.56	2.32	$P\bar{1}$
$Rb_2InInBr_6$	5	-0.94	Γ	-0.94	18.81	$P\bar{1}$
$Rb_2TlTlBr_6$	5	-0.97	Γ	-0.97	28.50	$P\bar{1}$

Table S6 – continued from previous page

Formula	Category	F_{min}	q-point	$F_{min,\Gamma}$	ΔE	spacegroup
$Cs_2TlTlBr_6$	5	-0.70	Γ	-0.70	6.81	$P\bar{1}$

References

(S1) Travis, W.; Glover, E. N. K.; Bronstein, H.; Scanlon, D. O.; Palgrave, R. G. On the Application of the Tolerance Factor to Inorganic and Hybrid Halide Perovskites: a Revised System. *Chem. Sci.* **2016**, *7*, 4548–4556.

(S2) Dronskowski, R.; Bloechl, P. E. Crystal Orbital Hamilton Populations (COHP): Energy-resolved Visualization of Chemical Bonding in Solids Based on Density-functional Calculations. *J. Phys. Chem.* **1993**, *97*, 8617–8624.

(S3) Deringer, V. L.; Tchougréeff, A. L.; Dronskowski, R. Crystal Orbital Hamilton Population (COHP) Analysis As Projected from Plane-Wave Basis Sets. *J. Phys. Chem. A* **2011**, *115*, 5461–5466.

(S4) Maintz, S.; Deringer, V. L.; Tchougréeff, A. L.; Dronskowski, R. Analytic Projection from Plane-wave and PAW Wavefunctions and Application to Chemical-bonding Analysis in Solids. *J. Comput. Chem.* **2013**, *34*, 2557–2567.

(S5) Maintz, S.; Deringer, V. L.; Tchougréeff, A. L.; Dronskowski, R. LOBSTER: A Tool to Extract Chemical Bonding from Plane-wave Based DFT. *J. Comput. Chem.* **2016**, *37*, 1030–1035.

(S6) Zhao, X.-G.; Yang, J.-H.; Fu, Y.; Yang, D.; Xu, Q.; Yu, L.; Wei, S.-H.; Zhang, L. Design of Lead-Free Inorganic Halide Perovskites for Solar Cells via Cation-Transmutation. *J. Am. Chem. Soc.* **2017**, *139*, 2630–2638.

(S7) Volonakis, G.; Haghighirad, A. A.; Milot, R. L.; Sio, W. H.; Filip, M. R.; Wenger, B.; Johnston, M. B.; Herz, L. M.; Snaith, H. J.; Giustino, F. $Cs_2InAgCl_6$: A New Lead-Free Halide Double Perovskite with Direct Band Gap. *J. Phys. Chem. Lett.* **2017**, *8*, 772–778.

(S8) Xiao, Z.; Du, K.-Z.; Meng, W.; Wang, J.; Mitzi, D. B.; Yan, Y. Intrinsic Instability of $Cs_2In(I)M(III)X_6$ (M = Bi, Sb; X = Halogen) Double Perovskites: A Combined Density Functional Theory and Experimental Study. *J. Am. Chem. Soc.* **2017**, *139*, 6054–6057.